ISSN: 2633-4828 Vol. 5 No.2, June, 2023

International Journal of Applied Engineering & Technology

ANALYSIS AND EVALUATION OF BLIND IMAGE RESTORATION

Somesh Kumar Dewangan[1] Dr. Siddhartha Choubey[2] Dr. Jyotiprakash Patra[3] and Dr. Abha Choubey[4]

[1]Ph. D. Research Scholar, [2]Associate Professor (SSTC-SSGI), [3]Associate Professor (CSVTU Bhilai), [4]Associate Professor (SSTC-SSGI)

[1, 2, 4] Computer Science and Engineering, Shri Shankaracharya Technical Campus- Shri Shankaracharya Group of Institutions

Bhilai (Chhattisgarh), India

[3]Computer Science and Engineering, Chhattisgarh Swami Vivekanand Technical University, Bhilai (Chhattisgarh), India

Received: 02 March, 2023 Revised: 05 May, 2023 Accepted: 21 May, 2023

ABSTRACT

Dazzle image reconstruction finds wide-ranging applications in fields such as astronomical imaging and clinical imaging for remote sensing. The objective of blind image restoration is to recreate the original image from a corrupted perception without prior knowledge of either the genuine image or the degradation process. One prevalent method in blind deconvolution is the category of techniques that execute the blind convolution by estimating the Point Spread Function (PSF) predating the restoration. Motion blur represents an inevitable trade-off between the degree of blur and the noise level in the captured image. The effectiveness of any restoration algorithm typically depends on these factors, making it challenging to find the optimal balance for ease of the restoration process. This paper discusses the concept of PSF identification and image restoration using various blind deconvolution algorithms."

Keywords: Motion Blur, Noise, PSF

INTRODUCTION

In various fields such as astronomical imaging, sonar imaging, remote sensing, clinical imaging, microscopy, and photography, images often present a noisy and obscured rendition of the original scene. Analyzing such images involves techniques capable of discerning shades, colors, and relationships imperceptible to the naked eye. This typically concerns images in bitmap formats, scanned in or captured with digital cameras. Restoration becomes crucial to reconstruct or recover an image that has been corrupted, leveraging inferred information about the degradation phenomenon. Let's denote this as:

$$g=Hf+n$$

There are two primary strategies for image restoration: non-blind restoration and blind restoration. The non-blind restoration system aims to reconstruct the original image "F" from the degraded image "G" and the Point Spread Function "H". It involves accurately estimating the blurring and distortions caused by the image system. However, when dealing with images of moving subjects where parameters like shutter speed or subject frequency are unknown, restoring a "blind" image becomes exceedingly challenging. In such cases, obtaining both "F" and "H" simultaneously becomes necessary using available information.

Several methods exist for incorporating prior information into the subframes "f" and "H". One approach involves imposing constraints on the convex cluster for successful execution. Another method imposes arbitrary constraints on the a priori distribution of the Bessie framework. Blind correction strategies in the literature can broadly be categorized into two types:

1. Strategies aimed at decomposing the degradation process into an unmodified process, such as zero separation, maximum likelihood (ML), and maximum a posteriori (MAP) approaches.
2. 2. Strategies combining blur detection and acquisition.

The blind Expectation-Maximization Algorithm (EMA) low-probability optimization approach is recommended for computing the PSF before imaging, preferred over combined methods. The primary objective is to transition from kernel to image resolution using the MAPk approach, with minor modifications to the MAPx algorithm. The significant difference lies in the kernel update software, which computes the covariance around the current background image, facilitating an efficient estimate of the distribution without additional computational effort. The algorithm situates MAPk in the expected minimized frame, with the key variable being a clear image.

Iterative ophthalmic algorithms, such as those developed by Ayers and Blind, are programmed to compute noise in both the image and frequency domain, facilitating the separation of two helix functions. Guidelines for restoring the maximum likelihood estimate are provided for high-quality image analysis with minimal processing time. Abdul Karim's KL deviation method for blind image restoration visually displays the image restoration by minimizing the KL (Kullback-Leibler) difference between the substrate and the set of ideal shell distributions.

Additionally, an end system is implemented and assembled for straightforward double reduction, while Philippe and Jean pioneered the use of the MC scaling algorithm (MC-AM) with an EVAM state matrix and isotropic reduction technology, achieving a subtle balance and powerful noise suppression capabilities.

The Basic system is define following:

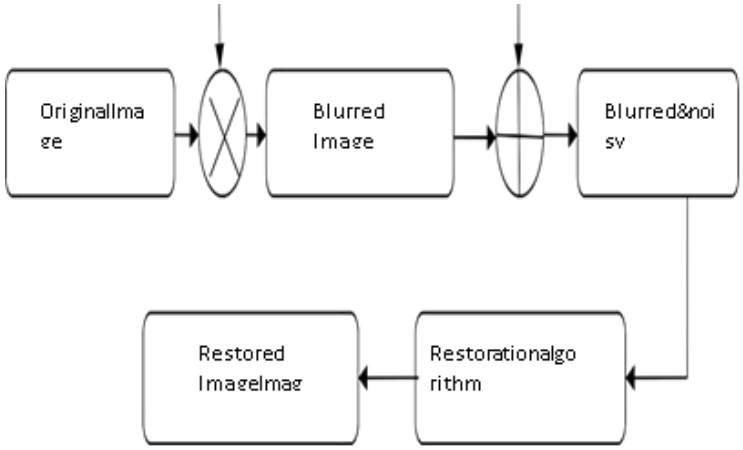

Figure1: Block Diagram for Blind Image Restoration

METHODOLOGY:

A: Duplicate Blind Decomposition Blind:

Non-negative visual phenomena often manifest in the context of superposition algorithms. Examining the entire image is crucial not only for assessing performance effectively but also for defining the energy calculation, which can be expressed as follows:

$f_i'(x) = f_i(x), f_i(x) \geq 0$

$f_i(x) = 0$ otherwise

$E = \int_{-D}^{+D} [f_i(x) - f_i'(x)]dx$ …….(ii)

$f_i(x) = f_i'(x) + \frac{E}{N}$……(iii)

However, the process is iterated, including the repetition of the Fourier sphere constraint. This ensures that any erroneous components are accounted for in the computation of significant events. The functions Fiu and the calculated (C(u) / Gi(u)) are obtained through the application of Fourier sphere restrictions. The Fourier sphere approach can be summarized as follows:

$$l\,C(u)l < noise\ level, \qquad F_{i+1}(u) = \tilde{F}_i(u)$$

$$l\tilde{G}_i(u)l \geq l\,C(u)l$$

$$F_{i+1}(u) = (1-\beta)\tilde{F}_i(u) + \beta\frac{C(u)}{\tilde{G}_i(u)}$$

$$l\tilde{G}_i(u)l < l\,C(u)l$$

$$\frac{1}{F_{i+1}(u)} = \frac{1-\beta}{\tilde{F}_i(u)} + \beta\frac{\tilde{G}_i(u)}{C(u)} \qquad \text{.....(iv)}$$

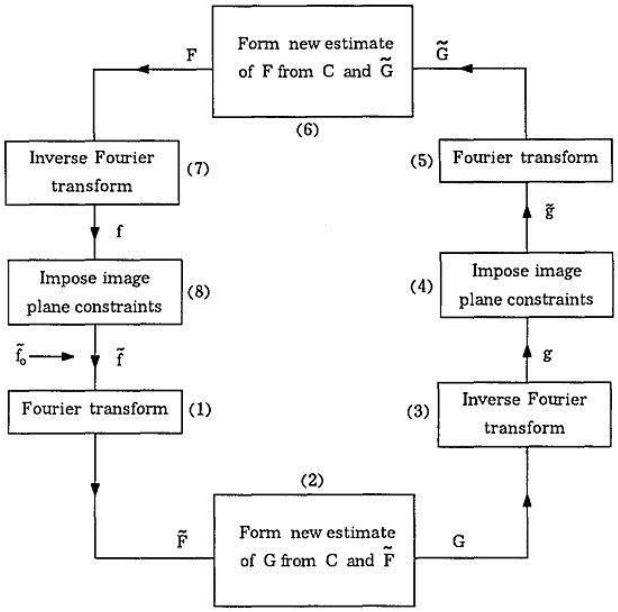

Figure 2: **Deconvolution Algorithm**

B. Maximum Likelihood Deconvolution

Maximum Likelihood Deconvolution (MLD) is an advanced optimization technique utilized for estimating the quantum of degradation caused by random noise. Image reconstruction is achieved through three microscope modes: wide-field epifluorescence, bright-field luminescence, and confocal fluorescence microscopy. The general flowchart of MLD, depicted in Figure 3, is outlined below. In this diagram, $o(k)$ represents the estimated value of the real image for the k-th iteration, $h(k)$ denotes the refined Point Spread Function (PSF) for the k-th iteration, and signifies the transposition operator.In the first stage, an initial estimation is made for the real image o(0)(,)$o(0)(x,y)$ and the PSF $h(0)$(x,y)$h(0)(x,y)$. Stage 2 proceeds based on the optimization method specified by the maximum-optimization algorithm. Stage 3 imposes reasonable constraints on the refined image and PSF response.

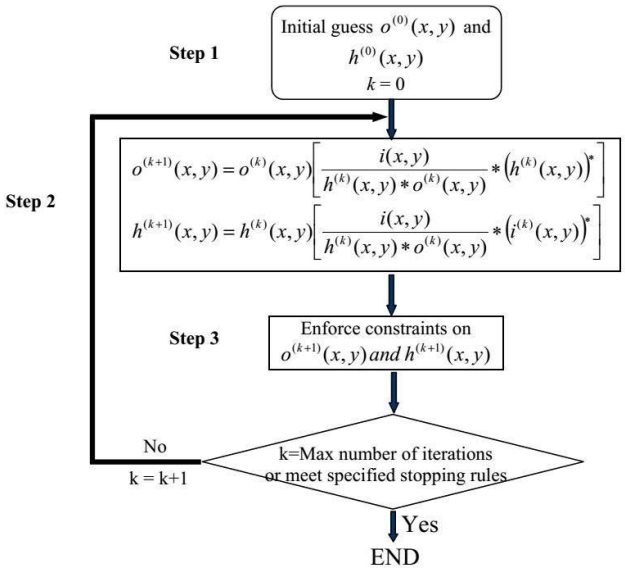

Figure 3: **Flow chart for MLD Algorithm**

C. Multichannel Blind iterative image restoration

The blind image MC essential minimization algorithm employs a point vector-based system to restore low figures. This technology utilizes a cell-centered, non-uniform discretization scheme, yielding tailored outcomes for the entire volition and Mumford-Shah schemes, known for noise reduction. The MC-AM algorithm is robust even under lower Signal-to-Noise Ratio (SNR) conditions, ensuring the reliability of these recovery methods. Each iteration of the EM algorithm incrementally enhances the probability function until it converges to the optimal point. These iterations progressively converge towards the unknown object, thus providing a robust starting point for the recovery process.

$$E(u,h)=\frac{1}{2}\sum_{p-1}^{p}\| h*u-z \|^{2}+\lambda Q(u)+\gamma R(h)\text{t.} \qquad \text{..... (v)}$$

The following table represents:-

S.No.	SNR	PMSE(h)	PMSE(u)
1.	60dB	2.23	1.30
2.	45dB	5.86	3.15
3.	35dB	12.34	5.14
4.	25dB	22.4	10.84
5.	15dB	42.77	20.75

Table 1: Show the value of image and blur

D. KL divergence approach

The prediction of both original and empty images involves minimizing the Kullback-Leibler deviation between probability distributions in the observed data. The default image, offered as a packaged option, caters to variables, facilitating a straightforward but iterative process that requires multiple repetitions to converge. Employing double reduction of the KL distance helps minimize the distinction between the perceived image distribution and the original image distribution.

Once the turbidity is established, a series of tests are conducted on a set of three components: the X-view and fuzzy parameter set, denoted as TTS, along with control parameters and alpha. The TTS is a parameter set represented as TTS=[x,y,T]TTS=[x,Ty,T], where t is determined.

$(p,\theta)_{ML} = arg_{min} KL(p(x,y) \parallel q(y,x;\theta)$..... (vi)

Following table present ISNR Value

S.No.	Images with noise	ISNR
1.	Image1(29dB)	1.59
2.	Image2(49dB)	2.22

Table 2: The value of ISNR

B. **Marginal Likelihood Optimization**:
This method comprises the following steps:

1. Obtain a blurred photo of the scanned image.
2. Introduce Gaussian noise.
3. Determine the Point Spread Function (PSF), also known as the kernel, of the degraded image.
4. Utilize the MAPP method to recover and identify the optimal "E" for the given image.
5. Employ an Expectation-Maximization (EM) algorithm to reconstruct the image on a single core.
6. Evaluate the performance of image retrieval by computing the Peak Signal-to-Noise Ratio (PSNR), Universal Image Quality Index (UIQI), and quality (Q) components.

The obtained values for PSNR, UIQI, and Q for the reconstructed result are 33.158, 0.889, and 49.75, respectively.

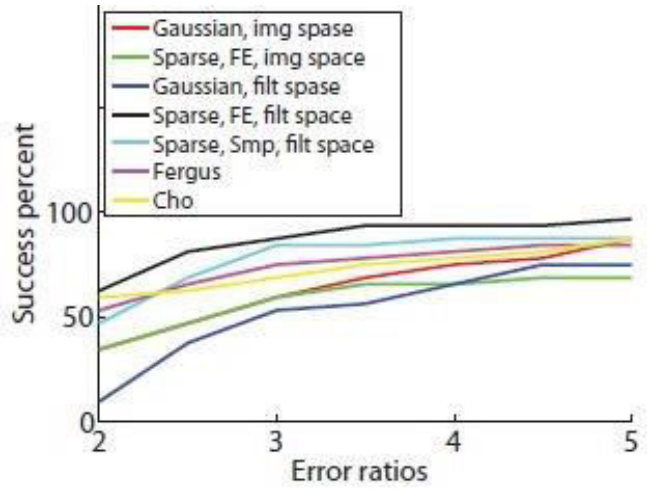

Figure 4: **Histogram of the error ratio**

E. MAP & HMRF Extractor
The Blind Pro method employs various estimation techniques to tackle PSF-based evaluation methods and local perceptual obscuration, while addressing PSF parameters and image restoration for smooth images. It utilizes Hoover Markov's previous model for this purpose.

PSF Estimation: The PSF is represented as a square logo, and it's crucial to estimate both the horizontal and vertical scales. Damaged images and obscured images are filtered to focus on the image edges' locations, aiding in defining the PSF medium. The PSF assistant can be identified through a reference image.The determination of the PSF support is outlined as follows:

V_size= $arg_m \min(J(m,0))$

h_size=$arg_n \min(J(0,n))$

Where v_sizendh_size are the estimated blur support in the vertical and horizontal directions, respectively J(m,n) is the autocorrelation of the image and it is defined by

The blur support in the vertical and horizontal directions, denoted by *vsize* and *hsize* respectively, are estimated parameters. The autocorrelation of the image, represented by *J*(*m*,*n*), is defined as:

$$J(m,n) = \frac{1}{(N-m)(M-n)} \sum_{x=n}^{N-1} \sum_{y=m}^{M-1} f(x,y) * f(x-n,y-m) \quad \text{.....(vii)}$$

Estimation of restored Image:

The quality of the image increases as the Q value rises. When operating in automatic mode, three metrics—PSNR, UIQI, and MetricQ—are computed. Alternatively, the MAP and HMRF methods yield superior results. In silent mode, the original image is convolved with a Gaussian blur of *H*=2.1. If noise mode is selected, the input image will be subject to additional noise. Table 3 below showcases the performance of different virtual image restoration techniques under silent mode

$$p(f) = \frac{1}{Z_f} \exp\{ -\frac{1}{T_f} \sum_{c \epsilon C} \rho_a (d_\epsilon^t f) \quad \text{.....(viii)}$$

Where Z_f *is normalization constant* T_f *is temerature*

parameter, c *is the clique of*

image pixels, C *is an assembly of* c *and*

$\rho(*)$ *is Huber function*

Using PSF to estimate image restoration is a two-step process. Create the objective function first and then go through the optimization

$$\rho_a(x) = \begin{cases} x^2, |x| \le a \\ 2a, |x| - a^2, |x| > a \end{cases}$$

process.

The Probablity density function of PSF is given by

$$p(h) = \frac{1}{Z_h} \exp\{ -\frac{1}{T_h} \sum_{c \epsilon C} \rho_a (d_\epsilon^t h) \quad \text{.....(ix)}$$

The minimum cost function is given by the equation

$$\check{f}\check{h} = argmin\{\|g - Hg\|_2^2 + \lambda \sum_{m=1}^{M} \sum_{n=1}^{N} \sum_{i=1}^{4} \rho_a(d_{m,n,i}^t f) + \gamma \sum_{m=1}^{P} \sum_{n=1}^{Q} \sum_{i=1}^{4} \rho_{a'}(d_{m,n,i}^t h)\}$$

.(x)

As the first element of Blind ProI, f represents the fidelity of the restored image in relation to the observation data "g". This term minimizes the noise amplification caused by poor fuzzy operator conditions.

Step 1: Set up the appropriate vector.

Step 2: Calculate the step size and update the image.

Step 3: Update the gradient and cost performance.

Step 4: Calculate the step size and update the conjugate vector of the image.

Step 5: Tool Update

Step 6: Complete the duplicate if the calculated value is less than the provided value. Otherwise, keep repeating.

PERFORMANCE ANALYSIS

The greater the Q value, the higher the image quality.In automatic mode and automatic mode, three standards are calculated, namely PSNR, UIQI, and MetricQ. Otherwise, the MAP and HMRF methods will provide better results. In silent mode, the original image is superimposed with a Gaussian blur of H = 2.1.The input image will be captured in noise mode. Table 3 below illustrates the restored performance obtained by various silent mode virtual image restoration techniques.

Table 3: Values of three metrics for different deconvolution methods (Noise free case)

Image	Noise free case		
	PSNR	UIQI	Q
Low image	21.622	0.899	39.96
Ibd method	28.332	0.875	46.85
MLD method	27.655	0.879	43.22
MLO method	30.232	0.895	48.72
MAP & HMRF method	30.433	0.895	49.32

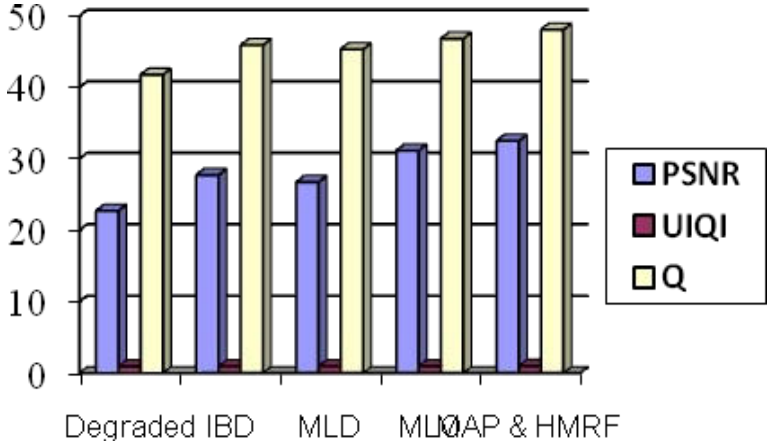

Figure 5: Noise

The Table 4 presented the quality of restored image gaining with the help of different different types of blind image restored techniques. Showing the result through graph.

Image	Noisy case		
	PSNR	UIQI	Q
Low Image	20.999	0.836	19.79
IBD method	23.112	0.839	31.93
MLD method	21.737	0.838	26.56
MLO method	24.131	0.866	38.23
MAP &HMRFmethod	24.321	0.865	45.52

Table 4: three metrics (Noisy)

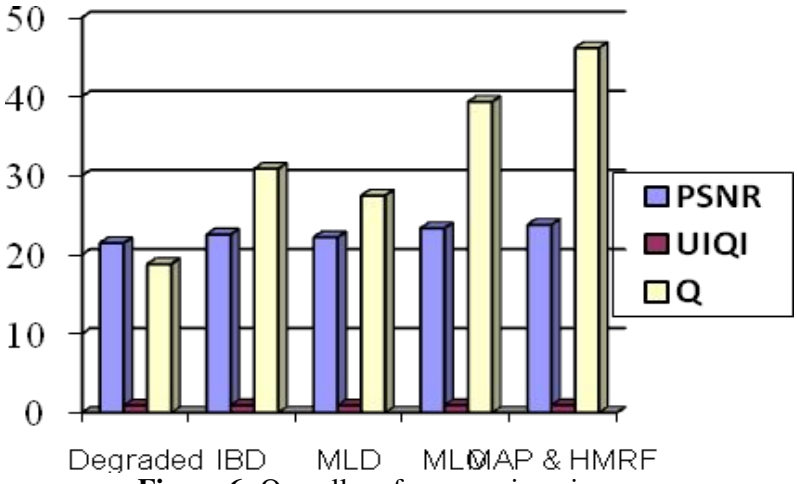

Figure 6: Overall performance in noisy case

CONCLUSION

This article presents several effective techniques for blind image restoration. As discussed earlier, it is evident that the MAP and HMRF strategies outperform other methods in restoring rural images based on metrics such as PSNR, UIQI, and Q. Interestingly, despite their effectiveness, the computational requirements of these strategies are comparable to those of the IBD and MLD methods.

REFERENCE

1. A. Levin, Y. Weiss, F.Durand, and W. T. Freeman, "Efficient marginal likelihoodoptimization in blind deconvolution", in proc. IEEE CVPR, 2011, pp.2657-2664.
2. G.AyersandJ. Dainty,' Iterativeblinddeconvolutionmethodanditsapplications,*'Opt.LETT.*,vol.13,no.7,pp.547-549,Jul.1988.
3. D.Fish,A.Brinicombe,E.Pike,andJ.Walker,"BlinddeconvolutionbymeansoftheRichardson-Lucyalgorithm",*J.Opt.Soc.Amer.A,Opt.ImageSci.,*vol.12,no.1,pp.58-65,Jan.1995.
4. T.J.Holmes,S.Bhattacharyya,J.A.Cooper,D.Hanzel,V.Krishnamurthi,W.Lin,B.Roysam,D.H.SzarowskiahdJ. N. Turner, "Light microscopic images reconstructed bymaximumlikelihooddeconvolution",in*HandbookofBiological confocal Microscopy*. Berlin, Germany: Springer-Verlag, 1955,pp.389-402.
5. D.KundurandD.Hatzinakos,"Blindimagedeconvolution,"IEEE Signal Process. Mag., vol. 13, pp.43–64,1996.

6. M.M.Chang, A.M.Tekalp,andA.T.Erden,"Blur identification using bi-spectrum,"IEEE Trans. SignalProcess., vol. 39,no. 10,pp.2323–2325, Oct. 1991.

7. S. J. Reeves andR. M. Mersereau, "Bluridentificationbythemethodofgeneralizedcross-validation,"IEEETrans.ImageProcess.,vol.1,no.3,pp.301–311,Aug.1992

8. R.L.Lagendijk,J.Biemond,andB.E.Boekee,"Identification and restoration of noisy blurred images usingtheexpectation-maximizationalgorithm,"IEEETrans.Acoust., Speech Signal Process., vol. 38, no. 7, pp. 1180–1191,Jul.1990.

9. G.PavlovicandA.M.Tekalp,"Maximumlikelihoodparametricbluridentificationbasedonacontinuousspatialdomainmodel,"inProc.Int.Conf.Acoust.,Speech,Signal Process., 1991, vol. 4, pp. 2489–2492.

10. R. Fergus, B. Singh, A. Hertzman, S. T. Roweis, and W.Freeman,"Removingcamerafromasinglephotograph",ACM Trans.Graphics,vol.25,pp.787–794, 2006.

11. L.Lucy,"Bayesian-basediterativemethodofimagerestoration,"J.Astronomy,vol.79,pp.745–754,1974.

12. L.ChenandK.Yap."Efficientdiscretespatialtechniquesforblursupportidentificationinblindimagedeconvolution" ,*IEEEtrans.signalprocess*.,vlo.54,no.4,pp.1557-1562,apr.2006.

13. H.shen, L.zhang,B.Huang,andp.Li "A MAP approachforjointmotionestimation,segmentation,andsuperresolution",*IEEETrans.Image process*., vol.16,no.2,pp.479-490, Feb.2007.

14. L.Zang,Q.Yuvan,H.ShenandP.LI,"Multiframeimagesuper-resolution adapted withlocalspatialinformation",*J.,Opt.Soc.Amer.A,Opt.Image Sci*.,vol.28,no.3,pp.381-390,Mar.2011.

15. Abd-KrimSeghouane, "A kullback-LeiblerDivergenceApproach to blind image Restoration" IEEE Trans. ImageProcess., vol.20,no. 7,July2011

16. Filip ˇSroubek and Jan Flusser, Senior Member, IEEE,"MultichannelblinditerativeImagerestoration",IEEETranson ImageProcessing,vol:12,no:9,Sep 2003

17. Ma, K., Liu, W., Zhang, K., Duanmu, Z., Wang, Z., & Zuo, W. (2017). End-to-end blind image quality assessment using deep neural networks. *IEEE Transactions on Image Processing*, *27*(3), 1202-1213.

18. Bigdeli, S. A., & Zwicker, M. (2017). Image restoration using autoencoding priors. *arXiv preprint arXiv:1703.09964*.

19. Li, L., Pan, J., Lai, W. S., Gao, C., Sang, N., & Yang, M. H. (2019). Blind image deblurring via deep discriminative priors. *International journal of computer vision*, *127*(8), 1025-1043.

20. Helminger, L., Bernasconi, M., Djelouah, A., Gross, M., & Schroers, C. (2020). Blind Image Restoration with Flow Based Priors. *arXiv preprint arXiv:2009.04583*.

21. Jiao, J., Tu, W. C., Liu, D., He, S., Lau, R. W., & Huang, T. S. (2020). Formnet: Formatted learning for image restoration. *IEEE Transactions on Image Processing*, *29*, 6302-6314.

22. Mao, X. J., Shen, C., & Yang, Y. B. (2016). Image restoration using convolutional auto-encoders with symmetric skip connections. *arXiv preprint arXiv:1606.08921*.

23. Nagata, T., Motohashi, S., &Goto, T. (2018, November). Blind image restoration of blurred images using failing detection process. In *2018 IEEE Global Conference on Signal and Information Processing (GlobalSIP)* (pp. 16-20). IEEE.

24. Bi, X. J., & Wang, T. (2008, May). Adaptive blind image restoration algorithm of degraded image. In *2008 Congress on Image and Signal Processing* (Vol. 3, pp. 536-540). IEEE.

25. Hongo, M., &Goto, T. (2020, October). Learning-based Image Restoration Method for Blurred License Number Plate Images. In *2020 IEEE 9th Global Conference on Consumer Electronics (GCCE)* (pp. 111-112). IEEE.

26. [26] Fatima H.R., Madhan K (2014) Evaluation of Blind image Restoration International Journal of Advanced Research in Computer Engineering & Technology (IJARCET) Volume 3 Issue 12, December 2014